COASTAL MULTI-HAZARD VULNERABILITY ATLAS

INDIAN NATIONAL CENTRE FOR OCEAN INFORMATION SERVICES

MINISTRY OF EARTH SCIENCES, GOVERNMENT OF INDIA

HYDERABAD - 500 090

2022

DISCLAIMER

Multi-Hazard Vulnerability Mapping (MHVM) along the Indian Coast was carried out using data related to historical extreme water levels, historic shoreline change, sea level change, and high-resolution topographic data. After careful corrections, synthesis, and extensive GIS analyses, the multi-hazard vulnerability maps were finalized on a 1:25,000 scale for the Indian mainland, and Andaman and Nicobar Islands where high-resolution topographic data is available. These maps represent low-lying coastal areas exposed to oceanic hazards within 100 years return period.

These maps are intended to provide baseline information on the coastal zones vulnerable to coastal flooding due to oceanogenic hazards.

However, these maps are NOT meant to replace detailed scientific investigations that are mandatory/required to plan location-specific coastal activities.

While using the maps provided in the Atlas, the user agrees that INCOIS, MoES will not be liable for any direct or indirect loss arising from the use of the information.

Data used, methodology, accuracies and results are included in the atlas as reference material. While sufficient care has been taken to prepare MHVM maps and integrate information from various sources in a reliable manner for value addition in the maps, INCOIS/MoES disowns responsibility for any inadvertent errors beyond its limitations.

Appropriate use and conclusions drawn from these maps are the user's responsibility. These maps require expert interpretation and are intended to guide coastal administrators only and NOT for general public use.

INDIAN NATIONAL CENTRE FOR OCEAN INFORMATION SERVICES (INCOIS)

HYDERABAD 500 090

DOCUMENT CONTROL AND DATASHEET

Report No. & Date	:	INCOIS-OSAR-CGAM-CMV-2022-03
Title	:	Coastal Multi-Hazard Vulnerability Atlas
Type of the Report	:	Atlas and other documents
Pages & Maps	:	579 & 1054
Concept	:	Shailesh Nayak
Coordination	:	T. Srinivasa Kumar
Investigators	:	R. S. Mahendra Prakash Chandra Mohanty E. Pattabhi Rama Rao Sudheer Joseph T. M. Balakrishnan Nair
Originating Unit	:	Coastal Geospatial Application Mission (CGAM), Applied Research and Research to Operation Division (ARO), OSAR, INCOIS
Abstract	:	Multi-Hazard Vulnerability Mapping is a holistic approach to estimate the composite hazard line based on the synthesis of extreme water level, sea-level change, shoreline change rate and high-resolution topography in a GIS environment. These maps represent the coastal inundation due to oceanogenic disasters in 100-year recurrence. The mapping was carried out on 1:25,000 Scale covering the Indian mainland and Andaman & Nicobar Islands. The maps presented in this Atlas provide vital coastal zone management and planning inputs.
Keywords	:	Extreme Water Level; Sea-level Change; Shoreline Change; Hazards; Exposure; GIS
Security Classification	:	Restricted
Distribution by	:	INCOIS and NCCR, Ministry of Earth Sciences
Citation	:	Nayak, S., Srinivasa Kumar, T., Mahendra, R.S., Mohanty, P.C., Rao, E.P.R., Joseph, S. and Nair, T.M.B. (2022) Coastal Multi-Hazard Vulnerability Atlas. INCOIS-OSAR CGAM-CMV-2022-03, INCOIS, Ministry of Earth Sciences, Hyderabad, India.

FOREWORD

Coastal systems and low-lying areas experience adverse impacts of sea-level rise such as submergence, coastal flooding, and coastal erosion. Urbanization and the rapid growth of coastal cities have led to an increase in population in the past few decades resulting in the development of numerous megacities in all coastal regions around the world. In India, there are three coastal megacities Kolkata, Mumbai and Chennai. Most of the population growth in developing countries like India occurs in coastal urban settings. Such densely populated low-lying coastal urban zones are highly exposed to impacts of sea-level rise.

Climate change and accelerated sea-level rise also exacerbate the risks of extreme events such as storm surges, coastal erosion, high waves and tsunamis. As per the IPCC, AR5, the population and assets of humans and their properties are exposed to coastal risks. Further, it was reported that vulnerable people, human systems, and climate-sensitive species and ecosystems are most at risk due to extreme events, including coastal flooding (IPCC, AR6). However, an upward trend in Mean Sea Level and its projected increase by 2100 and beyond indicates that coastal systems and adverse impacts of extreme sea levels in low-lying coastal areas continue to increase. Coastal ecosystems are subject to many human-related or anthropogenic drivers. These coastal systems interact with climate-related drivers and confound efforts to attribute climate change impacts. Socio-Economic Development (SED) impacts the coastal system and influences the human population and the value of assets exposed to coastal hazards.

Government officials and disaster managers responsible for coastal development need accurate assessments of coastal hazards to make informed decisions. In this direction, Coastal Multi-Hazard Vulnerability Maps (MHVM) are valuable tools in identifying the vulnerable coastal zones prone to inundation from ocean disasters. I am sure that this Atlas provides valuable information on the coastal zones exposed to oceanogenic vulnerability and for the timely initiation of management actions. Thus, it will go a long way in helping the scientific community and policymakers of the country.

I congratulate members of the Coastal Geospatial Application Mission Team, ARO-OSAR of INCOIS and Dr. T. Srinivasa Kumar for their painstaking efforts in successfully coming out with this Atlas. I would also like to record my deep appreciation for all those who have contributed to this project's success.

New Delhi
Date: 26 May 2022

M. Ravichandran

M. Ravichandran
Secretary, MoES

PREFACE

Climate change is predominantly a result of anthropogenic activities. Climate change is a complex global phenomenon and impacts vary locally. The climate change risks are significantly enhanced due to the overlap of cascading climate-related hazards. Global sea levels are rising across the globe at an alarming rate. These rising sea levels can exert pressure on the densely populated societies located in the low-lying coastal zones, exacerbating the existing coastal hazards that result in severe damage. Coastal zones of India are, therefore, under tremendous pressure from frequent inundations from ocean disasters and explosive growth in anthropogenic activities, including an ever-growing population. The enhanced intensity of the tropical cyclones and floods in tropical India due to climate change highlights the potential need for better adaptation and mitigation strategies. Hence, it is essential to understand the extent of coastal zones exposed to ocean disasters that can inundate and pose a threat.

In this regard, maps presented in the Atlas provide baseline information on the extent of the coastal inundation due to oceanogenic disasters that can cause inundation. We believe that these maps will serve as valuable tools for coastal zone management, especially for the natural disasters like storm surges, high waves and tsunamis that generate coastal inundation.

I congratulate Dr. Srinivasa Kumar and his team for bringing out this Atlas at an apt time to address the climate adversities along the coastal zones of India.

I am convinced that this Atlas provides the necessary impetus for understanding the coastal zones exposed to oceanogenic hazards and helps to initiate management plans. This Atlas shall also serve as input to the scientific community and decision-makers of the country.

Bengaluru
Date: 19 May 2022

SRNayak

Shailesh Nayak
Director, NIAS

PREAMBLE

Coastal zones are the confluence of air-sea-land processes. Low-lying coastal systems are primarily affected by flooding due to coastal erosion, submergence, sea-level rise, etc., which are exacerbated by climate change. The Intergovernmental Panel on Climate Change (IPCC), in its 5th assessment report (AR5) reported that the communities and assets are exposed to coastal risks.

Coastal zones are densely populated and more than 50% of the world's population is located up to 60 km from the coast (United Nations 1992). In the past four decades, enormous pressure has been witnessed along the coastal zones due to population growth and developments. Mean Sea Level (MSL) and its expected increase in the coming century suggest that low-lying coastal systems will continue to experience adverse impacts of extreme sea levels.

In view of this, a systematic coastal vulnerability assessment is imperative to coastal zone management and planning. The MHVM Atlas of the INCOIS, MoES is vital in providing baseline information for coastal disaster management. These maps provide vital inputs in making scientific decisions on developing resilient coastal communities.

I congratulate the team of scientists from INCOIS for generating this valuable Atlas on coastal multi-hazard vulnerability. I also thank the chairs and members of all the committees constituted to guide this project and painstakingly evaluated the deliverables.

We shall be delighted to receive feedback from the users about the utility of these maps. Comments and suggestions are helpful for further improving the content of these maps.

Hyderabad
Date: 26 May 2022

T. Srinivasa Kumar
Director, INCOIS

ACKNOWLEDGEMENTS

The investigators are highly indebted to **Dr. M. Ravichandran**, Secretary, MoES, Government of India, for his support and encouragement. Thanks to **Dr. Shailesh Nayak**, former Secretary, MoES and Director, NIAS, Bengaluru, for his keen interest in providing his conceptual ideas and guidance throughout the work.

We thank **Dr. T. Srinivasa Kumar**, Director, INCOIS, for providing all scientific facilities and encouragement. He coordinated the project from its inception, and we thank him for his contribution to the successful completion of the work. We express our gratitude to **Dr. S. S. C. Shenoi**, Former Director, INCOIS, for providing constant encouragement and facilitating the project.

Sincere thanks to Project Management Committee constituted to guide this project under the chairmanship of **Dr. Y. V. N. Krishnamurthy**, Former Director NRSC and **Dr. V. Bhanumurthy**, Former AD, NRSC. Thanks to all the project management committee, subcommittee, and map vetting committee members for their valuable guidance throughout the project. Thanks to NCCR, NCESS, NRSC and ADRIN for providing the services of the experts who helped in technical guidance.

Our colleague **Shri. B. V. Satyanarayana** was a member of the PMC and the sub-committee that assisted in implementation of this project and his contribution is gratefully acknowledged.

The authors thank **Mr. H. Shiva Kumar** and **Mr. Satej Panditrao**, Project Assistants, who helped to generate the map composites. We thank our colleague **Dr. T. V. S. Uday Bhaskar**, Scientist F, for valuable discussions on return period calculations.

We also thank **Mr. Hrusikesh Bisoyi**, CIFNET, Vizag and **Mr. Raghavendra Mupparthy**, NCMWRF, New Delhi, who helped us in this project in the initial stage. Thanks to our colleagues **Mr. Ch. Patanjali Kumar**, **Mr. N. Kiran Kumar**, **Dr. Aneesh Lotliker**, **Mr. K. Annapurnaiah**, **Mr. M. Nagaraja Kumar** and **Mr. R. Venkat Shesu** for their encouragement.

The authors would like to thank Global Observatory for Ecosystem Services (GOES), Michigan State University for the Landsat data, and Global Sea Level Observing System (GLOSS) for the sea level data. Thanks to USGS for making available Landsat data and Digital Shoreline Analysis Software (DSAS) on their website. Thanks to SRTM and ALOS-POLSAR project teams for making data available. Thanks to ESRI for making available topographic base maps on their map server. Thanks to the SRTM projects teams for making available topographic data on their website. Thanks to NOAA for making the sea level trends of Indian stations available online.

Finally, thanks to all who helped and encouraged this work.

Hyderabad
Date: 23 May 2022

T. M. Balakrishnan Nair
Group Director, INCOIS

Contents

List of Figures

List of Tables

1. INTRODUCTION

Though climate change is a global phenomenon, its impacts vary locally and accordingly; adaptive capacities, sensitivities, and strategies need to be worked out (Piya et al., 2012). The areas with dense populations and bio-diversity are most vulnerable. Livelihoods and economies of the coastal population are dominated by agricultural, pastoral, forest production systems and marine resources and may be highly sensitive to climate variations. Climate change can impact the production of these systems affecting income, the cost of production, supplies, commodities, food storage, livestock, financial savings and food security (Leary et al. 2008). Impacts of climate change are more severe in east, southeast and South Asia due to accelerated sea-level rise (Wong et al. 2014). Climate models suggest a rise in the intensity of tropical cyclones in the northern Indian Ocean basin during the 21st century (Krishnan et el., 2020). Climate change Besides, huge population and development pressure have been building in the coastal areas in recent decades, so the resources in this region are more susceptible and exposed to climatic hazards. Global climate change and accelerated sea-level rise exacerbate the already existing high risk of storm surges, severe waves, and tsunamis (Kumar et al. 2010) and make coastal communities vulnerable.

Coastal zones are significant regions of the confluence of natural marine and fluvial processes responsible for maintaining the coastal environment. Coastal systems and low-lying areas experience adverse impacts such as submergence, coastal flooding, and coastal erosion due to relative sea-level rise. The densely populated low-lying coastal zones are highly exposed to such events (Grases et al., 2020). As per the fifth assessment report (AR5) of the Intergovernmental Panel on Climate Change (IPCC) 2014, the population and assets of humans and their properties are exposed to coastal risks. Thus, human pressures on coastal ecosystems will increase significantly in the coming decades due to population growth, economic development, and urbanization (IPCC 2014; Wong et al. 2014). Sea-level rise in the northern Indian ocean was recorded at a rate of 1.06–1.75 mm/y during 1874–2004 and has accelerated to 3.3 mm per year in the last two and a half decades (1993–2017), which is comparable to the current rate of global mean sea-level rise (Krishnan et al. 2020). However, an upward trend in Mean Sea Level (MSL) and its projected increase by 2100 and beyond indicated that coastal systems and adverse impacts of extreme sea levels in low-lying coastal areas continue to increase. Extreme sea-level events are projected to occur frequently over the tropical regions (high confidence) and along the Indian coast (medium confidence) associated with an increase in the mean sea level and climate extremes (Krishnan et al. 2020). Coastal ecosystems are subject to many human-related or anthropogenic drivers (Halpern et al., 2008; Crain et al., 2009). Those interact with climate-related drivers and confound efforts to attribute climate change impacts. Socio-Economic Development (SED) impacts the coastal system and influences the number of people and the value of assets exposed to coastal hazards. The global population exposed to the 1-in 100-year extreme sea-level increased by 95% from 1970 to 2010. Nearly 70 million people and US$13 trillion worth of assets were exposed to a 100-year extreme sea level in 2010 (Jongman et al. 2012). Furthermore, the population exposed to the 1-in-100-year coastal flood is projected to increase from about 270 to 350 million in 2010 to 350 million in 2050 due to SED only (UN medium fertility projections) (Jongman et al. 2012).

India has been identified as one of the 20 countries that are most at risk of sea-level rise (Strauss and Kulp 2014). Observations suggest that the sea level has risen at an average rate of 2.5 mm/year along the Indian coastline since the 1950s (Rishi and Mudaliar 2014). A mean SLR of between 15 and 38 cm is projected by the middle of the 21^{st} century along India's coast. In addition, a 15 % projected increase in the intensity of tropical cyclones would significantly enhance the vulnerability of populations living in cyclone-prone coastal regions of India (Rishi and Mudaliar 2014).

1.1. MULTI-HAZARD VULNERABILITY MAPPING

One area may suffer from several natural hazards. Using individual maps to convey each hazard can be cumbersome for planners and decision-makers because of their number and possible differences in the area covered, scales, and detail. The primary objective of Multi-Hazard Vulnerability Mapping (MHVM) is to combine hazard-related information from different hazards in one map for a study area to convey a composite picture of the natural hazards of varying magnitude, frequency, and area of effect. MHVM may also be referred to as a "composite," "synthesized," and "overlay" of multi-hazard map.

Coastal inundation caused by various oceanogenic natural hazards such as cyclones, storms, tsunamis, and floods depends on the coastal elevation and slope. However, the inundation level varies depending on the intensity of the hazard. The inducing or triggering mechanism that can interconnect several hazards can be seen more easily through multi-hazard mapping. Characteristics of the natural phenomenon and its trigger mechanisms are synthesized from different sources and placed on a single map. The maps provided in this Atlas are holistic and represent the low-lying coastal areas exposed to oceanogenic hazards.

1.2. NEED AND SCOPE OF MULTI-HAZARD VULNERABILITY MAPS

Coastal regions of India are spread across nine maritime states, four union territories and the islands are considered one of India's four climate-sensitive regions (INCCA 2010). Economic developments encounter vulnerability as a system's predisposition to negative outwardness in terms of welfare loss (Rao et al., 2013). The vulnerability assessment is subjective and varies across the areas exposed to the intensities of climate change (Sehgal et al., 2017). Extreme sea-level events are projected to occur frequently over the tropical regions (high confidence) and along the Indian coast (medium confidence), associated with an increase in the mean sea level and climate extremes (Krishnan et al., 2020). Planning of appropriate actions for climate change requires a proper understanding of the spatial distribution of factors contributing to climate change vulnerability (Lee et al., 2015). The enhanced intensity of the tropical cyclones and floods in tropical India due to climate change highlights the potential need for better adaptation and mitigation strategies (Krishnan et al., 2020; Unnikrishnan et al., 2010).

Recognizing the significance of the coastal vulnerability to changing climate, the Government of India has launched the National Coastal Mission (NCM) as a sub-mission under the National Action Plan to Climate Change (NAPCC) to ensure that adaptive responses are appropriately built-in to deal with newer threats of climate change (NCM 2016). Hence, scientific assessment of coastal vulnerability is central to implementing national interventions for adaptation to climate change (Krishnan et al., 2019).

The maps provided in this Atlas generated on 1:25,000 scale serve as vital input for disaster management authorities to implement coastal disaster action plans. Further, these maps will also serve as the baseline information for understanding coastal zones exposed to oceanogenic hazards in a 100-years recurrence interval.

2. STUDY AREA

MHVM was carried for the landward side of the coastal zone from the shoreline up to the composite hazard line estimated in the current study, covering the entire coast of the Indian mainland, Andaman and Nicobar Islands (Figure 2). In the present study, the MHVM mapping was not carried out for the Lakshadweep Islands due to the non-availability of data.

3. DATA USED

The data used in the current study are derived from remote sensing, observatories and published literature, as given in Table 1.

Table 1. List of data used for the current study

Sl. No.	Parameter	Data Used	Resolution	Period
	Topography	ALTM	5m	2004-09
		Carto-DTM	10m	2005-08
		TerraSAR-X	18 m	--
		SRTM	30	--
		ALOS-PALSAR	30	--
1	Shore-line change rate	LANDSAT MSS	57 m	1972;
		LANDSAT TM & ETM	30 m	1989-2000
3	Extreme Water Level	Hourly Tide Data**	--	1871-2007**
		Published Literature*		
5	Sea-level change rate	GLOSS Data	---	1900-2005

* Historical Events of Extreme Water Levels Caused by Tsunami and Storm Surge from Published Literature.

**Tide Gauge data available for the 25 different tide gauges collected during 1880-2007 as shown in Figure1 pertaining to different periods.

Extreme water level: Extreme water levels pertaining to each tide gauge location were derived from the Survey of India (SOI) hourly tide data. Data from 1871 to 2007 were used to calculate extreme water levels and projected into the next 100 years based on the return period method. The hourly predicted tides were calculated using the Mike 21 software based on diurnal and semi-diurnal harmonic components. Locations of tide gauge stations are provided in Figure 1.

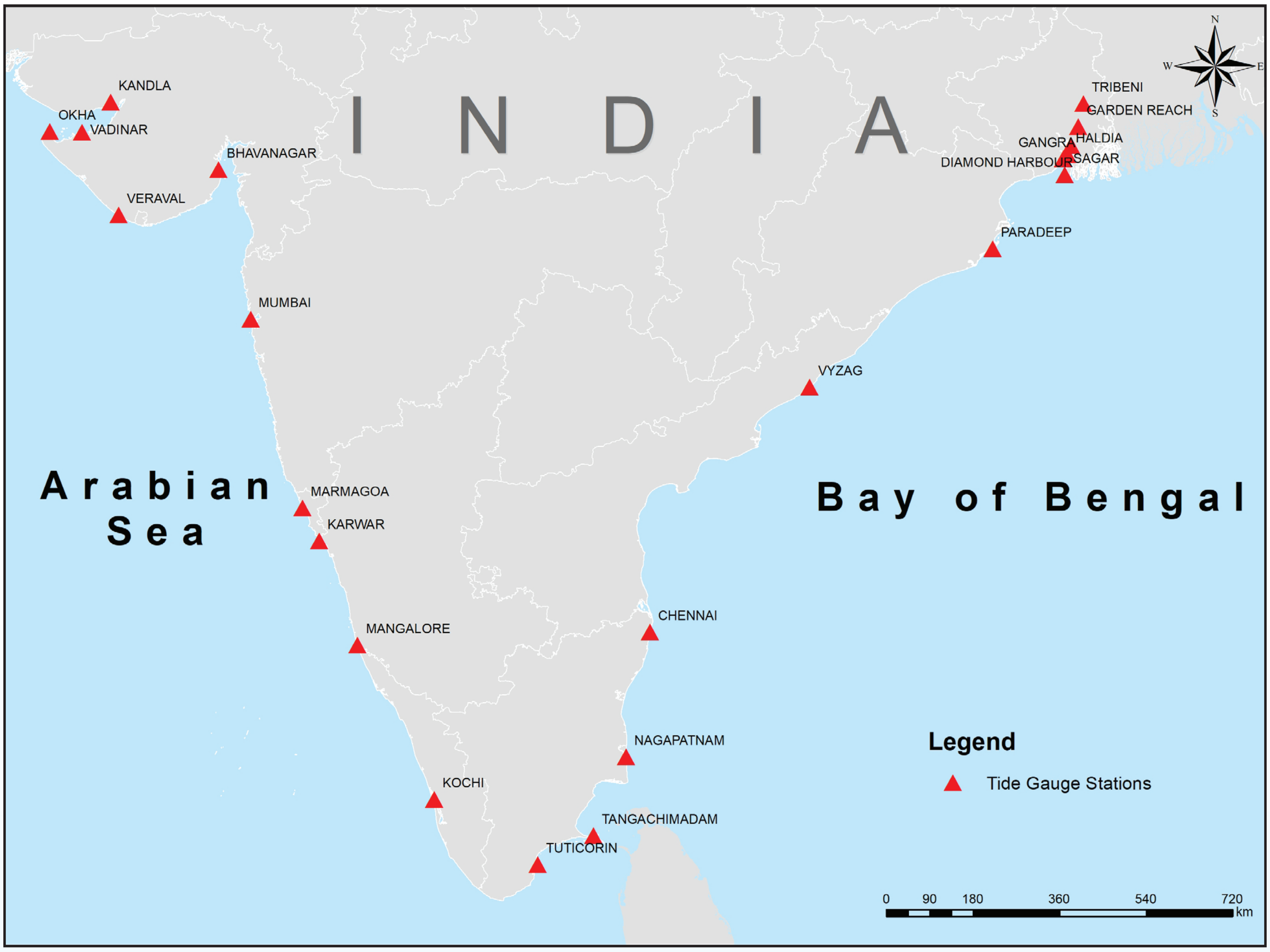

Figure 1. Location of Indian Tide gauge stations

Table 2. Availability of hourly tide gauge data for extreme water level calculations

Sl. No	Station	From Year	To Year	Duration (Y)	Availability (Y)
1	Chennai	1880	2007	127	101
2	Diamond Harbour	1874	2007	133	62
3	Gangra	1974	2006	32	31
4	Garden Reach	1949	2007	58	53
5	Haldia	1970	2007	37	33
6	Kandla	1952	2006	54	46
7	Karwar	1878	2006	128	34

8	Kidderpore	1873	1920	47	46
9	Kochi	1886	2007	121	71
10	Mangalore	1961	2006	45	39
11	Marmagao	1969	2007	38	30
12	Mumbai	1876	2006	130	120
13	Nagapattinam	1971	1990	19	18
14	Okha	1974	2006	32	32
15	Paradeep	1966	2007	41	40
16	Port Blair	1880	2007	127	61
17	Sagar	1951	1988	37	28
18	Tuticorin	1871	2007	136	36
19	Vadinar	1981	2006	25	26
20	Veraval	1959	1983	24	18
21	Vizag	1879	2007	128	50

Sea-level Change Rate: The long-term monthly mean Sea-level data pertaining to tide gauge stations shown in Figure 1 were downloaded from the Global Sea Level Observing System (GLOSS) network to calculate the Sea-level trend. The data availability of each tide gauge station is provided in Table 2.

Shoreline Change Rate: The Shoreline were extracted from Landsat Multi-Spectral Scanner (MSS) and Thematic Mapper (TM)/ Enhanced Thematic Mapper (ETM)/ Enhanced Thematic Mapper Plus (ETM+) with 56 and 30-meter resolution, respectively, in a different period from 1972 to 2001, to estimate the Shoreline change rate using Digital Shoreline Analysis System (DSAS) software.

Topography: Very high-resolution Airborne Lidar Terrain Mapping (ALTM) coastal elevation data with 5 meters spatial resolution was used up to 2 km from the coast. Beyond the 2 km, elevation data were derived using Cartosat-1 with 10 meters, spatial resolution was used. Further, Shuttle Radar Topographic Mission (SRTM) 30m spatial resolution data was used for the hinterlands of northern Odisha and West Bengal. Andaman and Nicobar area ALTM data were used for Port Blair, and in the remaining areas, the data from Cartosat-1 Digital Terrain Model (Carto-DTM), TerraSAR-X and data from Phased Array type L-band Synthetic Aperture Radar (PALSAR) onboard Advanced Land Observing Satellite (ALOS) (ALOS-PALSAR) data were being used. The spatial extents of the different topographic data used for the generation of MHVM maps are given in Figure 2.

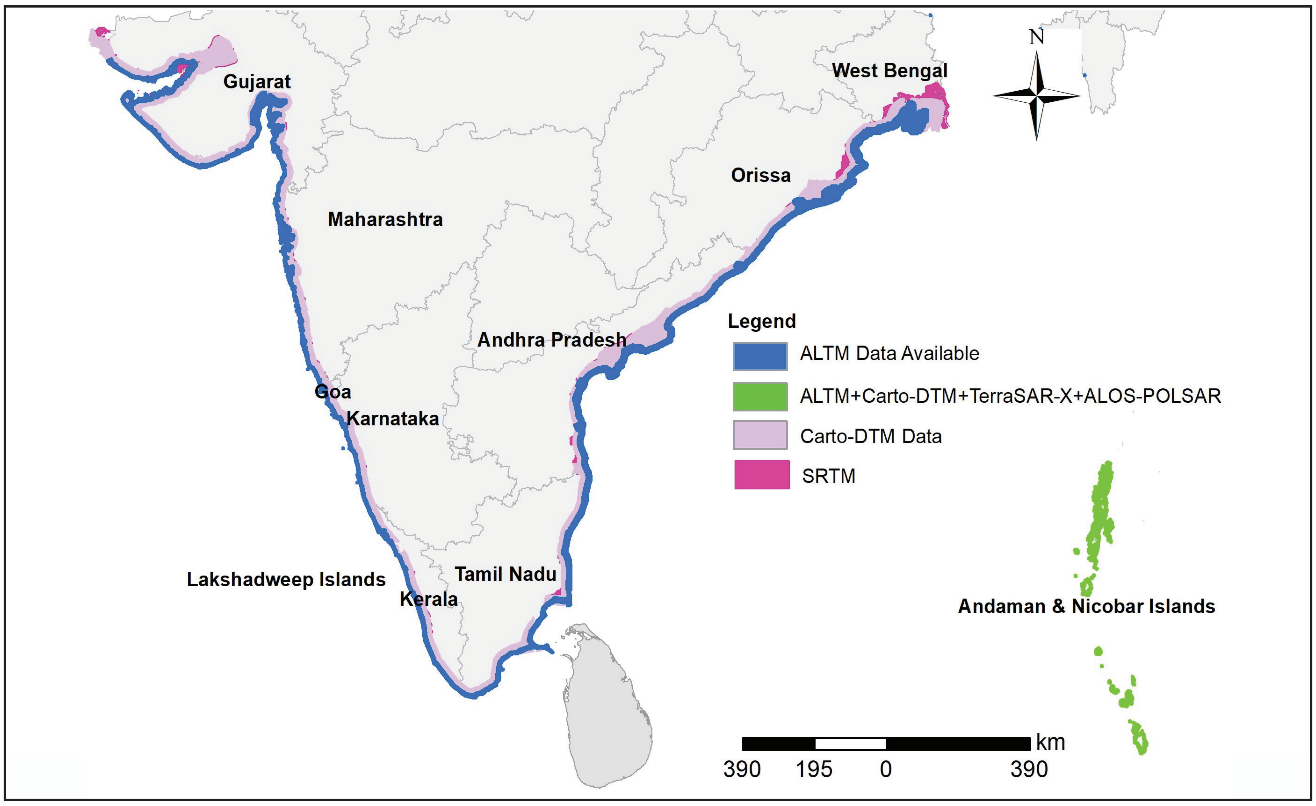

Figure 2. Spatial extents of the different topographic data used for mapping

4. METHODOLOGY

MHVM maps were prepared using the parameters: sea-levelchange rate; shoreline change rate; high-resolution topography, extreme water level & their return periods. The flowchart (Figure 3) shows the general methodology of the current study. The method used here is similar to Mahendra et al. (2010, 2011 and 2021).

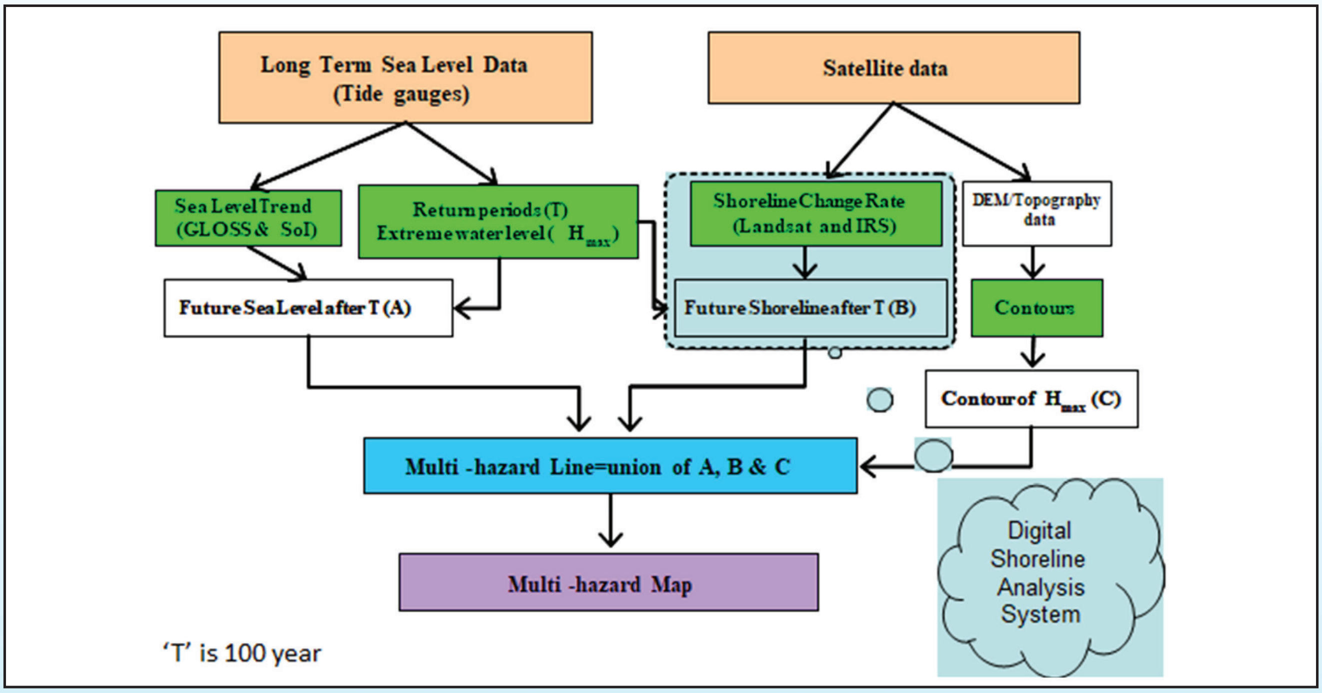

Figure 3. The flow chart depicting the current methodology

4.1. CALCULATION OF THE SHORELINE CHANGE RATE

Ortho-rectified Landsat MSS and TM images covering the coastline of the years 1970, 1980 and 2000 were downloaded from the Website www.landsat.org. The data has been projected to Universal Transverse Mercator (UTM) projection system with the WGS-84 datum. The shoreline along the coast was digitized using ArcMap 9.2 and ERDAS Imagine software using the on-screen point mode digitization technique. The Near-Infrared (NIR) band is most suitable for the demarcation of the land-water boundary (shoreline). The digitized shoreline for 1970, 1980 and 2000 in the vector format was used as the Digital Shoreline Analysis System (DSAS) to calculate the shoreline change rate (Mohanty et al., 2017; Mahendra et al., 2021). The inputs required for this tool are shoreline in the vector format, date of each vector layer and transect distance. The shoreline change rate is calculated for the entire study area.

4.2. CALCULATION OF THE SEA LEVEL TREND

The tide gauge dataset of the Global Sea-level Observing System (GLOSS) during the past century is used as the primary source of information for the sea-level trend in the study area. Tide gauge data recorded in 21 stations around the Indian Ocean, including Paradip, Sagar, Vizag, Chennai, etc., during the period from 1900 to 2005 is used to estimate the sea-level change rate by linear fit for all these tide gauge locations. Besides, sea level trends available from the NOAA website (URL: https://tidesandcurrents.noaa.gov/sltrends/) were also used.

4.3. ESTIMATION OF EXTREME WATER LEVELS AND RETURN PERIODS

Historical hourly tide gauge data recorded during the past century pertaining to 21 Indian tide gauges were used for calculating extreme water levels. The quality checks such as noise removal by using three sigma levels, data available more than 18hrs in a day and more than 75% of data available in a year were considered to avoid errors and bias. The quality passed data pertaining to all the stations were de-tided, and extreme water levels above astronomical tide were extracted using the Mike tide processing software.

The observed sea level (H) at any time could be considered as a composite of mean sea level (H_0), astronomical tidal components (H_{tide}), and perturbation term ($H\varepsilon$), which includes measurement uncertainty and contribution from an external force such as meteorological forcing (Pugh, 1987).

$$H = H_0 + H_{tide} + H_\varepsilon ------1$$

Where

$$H_{tide} = \sum_{i=1}^{n} H_{ai} cos(\omega_i t + \varphi_i) ------2$$

Where H_{ai} and φi, respectively, are amplitude and phase of i^{th} harmonic constituent corresponding to frequency ωi.

The components of amplitude and phase of major sixty tidal harmonic constituents (including annual and semi-annual harmonics) were derived from the hourly tide gauge data at each location using the least square-based Harmonic Analysis (Foreman, 1977) inbuilt in Mike 21 software developed by the Institute of Ocean Sciences (IOS). This IOS procedure is most suitable for decomposing non-continuous tide records into single long-term continuous data (Arjun et al., 2010; Adams et al., 2009). The astronomical contribution of the sea level time series was reconstructed using the amplitude and phase of all the semi-diurnal, diurnal, annual and semi-annual tidal harmonic constituents above Equation 2. The non-tidal residuals (Hε) were obtained by subtracting the tidal components (H_{tide}) from the original time series (H). The non-tidal residual tide data were used to extract yearly maximum extreme water levels and projected into the next 100 years based on the return period method. In addition to tide gauge data, the water levels recorded along the Indian coast due to earlier inundation events by tsunamis and storm surges were also taken from the published literature. These water levels were associated with the nearest tide gauge stations. The annual extreme water level and their return period for the next 100 years were calculated for each tide gauge station. The return period is calculated using the Extreme Value Distribution (EVD) function using the Grigorton probability of non-exceedance (Gringorten, 1963). The probability of the extreme water level in 100 years is assumed as the probable flooding level in the next 100 years. The details of the return period analysis were carried out based on mahendra et al. (2021), as detailed below.

Annual maximum water levels from residual water levels were extracted for each tide gauge station and tabulated in ascending order, and 'm' is the rank assigned to each sample from 1, 2, 3, ... N from low to high values of maximum water levels. The probability of non-exceedance (Gringorten 1963) was calculated to estimate the reduced variate as provided in Eq. 3:

$$P = \frac{m - 0\ 44}{N + 1 - 0.88} \text{----} = \frac{m - 0.44}{N + 0.12} - - - - - - 3$$

where 'm', is the rank of the sample in the increasing order of water levels and 'N' is the total number of samples. The reduced variate was calculated using the following equation (Eq. 4)

$$y = -\log_e(-\log_e p) - - - - - - 4$$

Annual extreme water levels observed versus reduced variate for all the stations were plotted to estimate the scale factor (a) and offset (u) based on the least square method. These scale factor and offset values were used to calculate the return periods. An example scatters plot of selected tide gauge stations was presented in Figure 4.

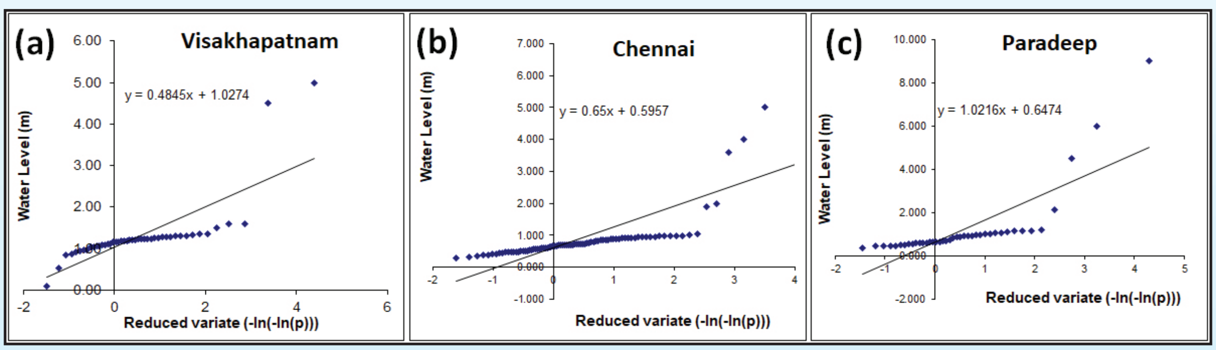

Figure 4. Example scatter plots of reduced variate and water levels for (a) Vishakhapatnam, (b)Chennai and (c) Paradeep stations.

The generalized extreme value (GEV) distribution function (Eq. 5) was used to calculate the extreme water levels in desired return periods:

$$U = u + a\{-\log_e[\log_e(1-\frac{1}{R})]\} - - - - - - -5$$

where 'U' is the extreme water level, 'R' is the return period in years, 'a' is the scale factor, i.e., slope value, and 'u' is the offset, a slope. The same exercise was repeated for all the stations and the extreme water level in a return period of 100 years was calculated (Figure 5).

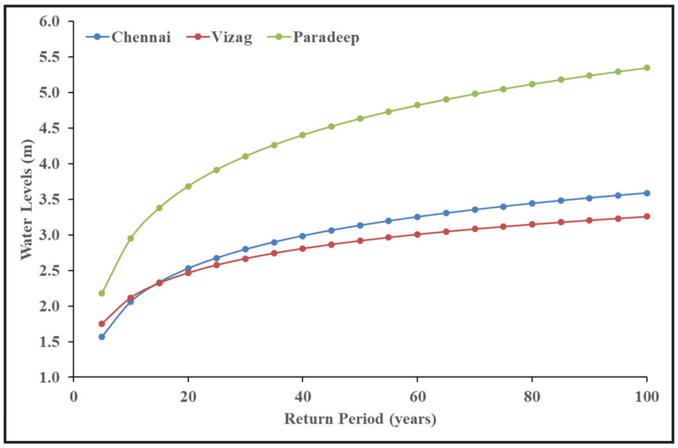

Figure 5. An example of return periods of extreme water levels plot of Chennai, Vizag and Paradeep stations showing expected extreme water levels and sea-level rise in 100 years.

4.4. GENERATION OF ELEVATION CONTOURS

The topographic data from the Airborne Lidar Terrain Mapping (ALTM) and Cartosat-1 Digital Terrain Model (DTM) and other sources mentioned in the data section were merged. Suitable interpolation and filters were applied to match at the edges to represent the continuous terrain optimally. Further, the contours of a 1-meter interval were generated. In the areas beyond these two data, the SRTM data was used for some areas, as shown in Figure 2.

4.5. GENERATION OF MULTI-HAZARD MAP

Sea-level change rate has been forecasted for the next 100 years based on the Sea Level Rise (SLR) rate. The future shoreline after 100 years has been drawn based on the rate of shoreline change. The estimated extreme water level and sea-level rise for each station were combined to estimate the probable maximum inundation expected in the next 100 years (flood line). The corresponding elevation contour line has been selected along the coastal zones representing the probable flood line based on this inundation level. The future shoreline position was estimated for the erosion sites to understand the possible impact of the erosion on the coast. The area between the coastline and the composite hazard line is the multi-hazard zone, composed of the inundation zone from extreme water levels caused by various oceanogenic disasters and erosion. The shapefile representing the multi-hazard zone and composite hazard line is overlaid on the base ESRI Topographic Maps and administrative boundaries. The maps presented in this Atlas are generated on 1:25,000 scale Survey of India (SOI) toposheet index.

4.6. LIMITATIONS AND ACCURACY OF MAPS

The actual limitation of these maps lies within the sensitivity of the data and the techniques used in the current study. The data gaps in the tidal observations might miss some events. The hourly tide data acquired from the survey of India tide gauges may slightly underestimate the actual amplitude, and minor events may get missed. However, the water levels observed during historical events from published data/literature included in the current study might supplement to fill gaps.

The high-resolution topographic data used from ALTM is very accurate and detailed. This data is available for the entire Indian mainland coast and up to 2 km from the coast, and few deltas cover beyond. Beyond these ALTM areas, Cartosat-1 DTM was being used to generate the MHVM. The ALTM data is highly accurate (vertical accuracy 35cm and 5m horizontal resolution) when compared to Cartosat-1 DTM (vertical accuracy 5m and Horizontal resolution of 10m) estimated using Ground Control Points (GCPs). The accuracy of the SRTM is of the order 3.82-5.85 m, and ALOS-POLSAR is 2.8-3.64 m, as reported by Zhang et al. (2019).

Adequate care has been taken to prepare MHVM maps and integrate information from various sources in a reliable manner for value addition in the maps. However, the SRTM data was used in the Odisha and West Bengal hinterlands to fill the gap of abruptly ending topographic data beyond the limitations of the 1:25,000 scale.

Further, these MHVM maps were validated with the Hudhudstorm surge inundation by comparing a similar scenario. The comparative results agree between storm surge inundation and corresponding MHVM scenarios along the open coasts. The maps underestimate the vicinities of the deltas and creeks due to fluvial influence from the land in case of cyclone-induced storm surge inundation.

5. RESULTS

The results of extreme water level and Sea-level change in the next 100 years for the tide gauge locations are provided in the following Table 3.

Table 3. Probability of Extreme water level/Flood level and sea level in 100 years

Station	Extreme Water Level (M)	Sea Level After 100Y (M) and Period of Data Used	Inundation/Flooding Level (M)
Chennai	3.59	0.055 (1916-2014)	4
Diamond Harbour	5.48	0.395 (1948-2014)	6
Gangra	6.63	0.2 (1974-2006)	7
Garden Reach	4.15	0.3 (1949-2007)	5
Haldia	4.25	0.283 (1970-2014)	5
Kandla	5.58	0.191 (1950-2013)	6
Karwar	2.49	0.103 (1970-2013)	3

Kidderpore	3.04	--	4
Kochi	1.72	0.154 (1939-2013)	2
Mangalore	2.29	0.3 (1961-2006)	3
Marmagao	3.29	0.145 (1969-2013)	4
Mumbai	3.4	0.08 (1878-2011)	4
Nagapattinam	4.68	--	5
Okha	2.93	0.13 (1975-2013)	4
Paradeep	5.34	0.194 (1966-2013)	6
Port Blair	5.65	0.22 (1916-1964)	6
Sagar	4.61	--	5
Tuticorin	2.61	0.054 (1964-2014)	3
Vadinar	3.95	--	4
Veraval	2.43	--	3
Visakhapatnam	3.26	0.105 (1937-2013)	4

-- Sea-level change rate is not considered due to incomplete data/negative trend

The multi-hazard vulnerability of the Indian coast based on the above inundation/flooding levels and future erosion is provided in Figure 6.

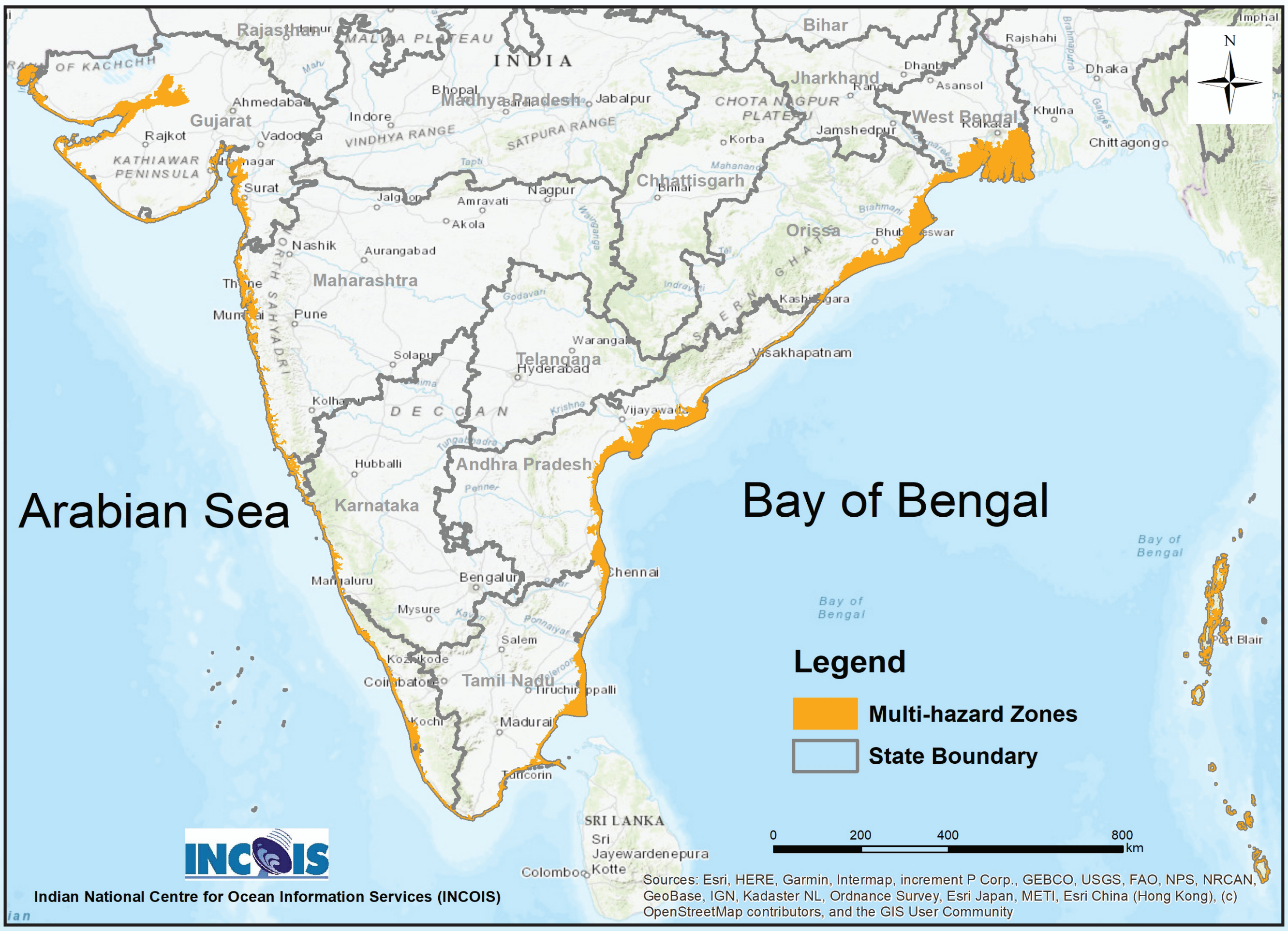

Figure 6. MHVM map of Indian Coast

5.1. GUJARAT

The MHVM map of the Gujarat coast, including Diu and Daman union territories, is presented in Figure 7. MHVM assessed in this study spans 17 coastal districts of Gujarat and two union territory regions of Diu and Daman, covering an area of 10525.21 km^2. Gujarat is India's northwestern state, associated with a long coastline and large low-lying areas, especially in the Kuchchh region and in the eastern parts of the Gulf of Khambat. The results of the MHVM assessment also reveal similar results recording maximum MHVM area in the Kuchchh district followed by Baruch, Jamnagar, Devbhumi Dwaraka and Surat districts (Table 4). The highest percent of the district's area covered under MHVM is Diu with 56.05%, followed by Baruch, Kachchh, Porbandar, Navsari and Devbhumi Dwaraka with 22.37, 15, 14.3, 13.37 and 13.01 percent respectively.

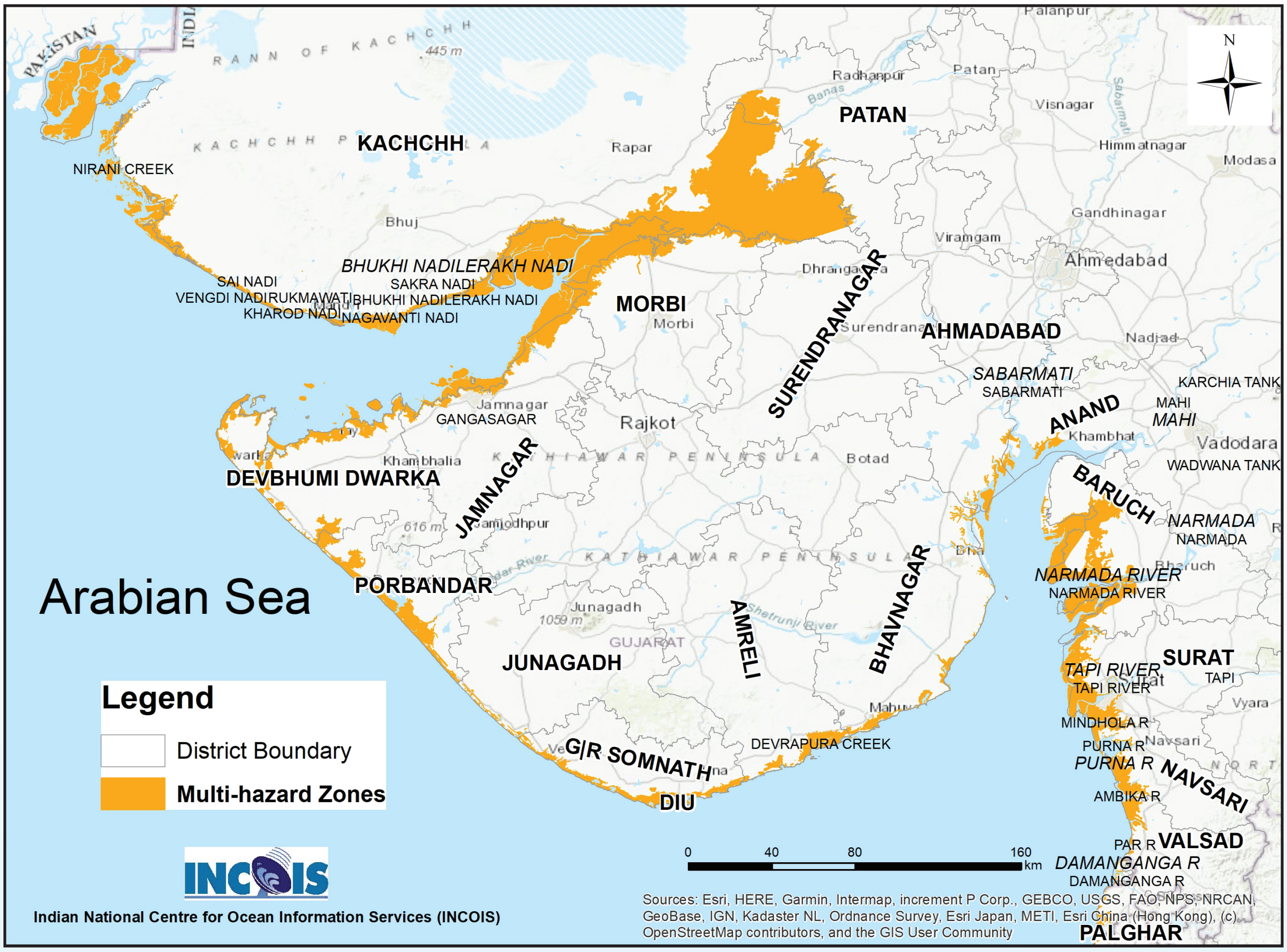

Figure 7. MHVM map of Gujarat coast

Gujarat coast is associated with large tidal amplitudes with 28,500 km^2 under the tidal influence that constitutes 62.3% of the country's total (Garg et al. 1998). This resulted in the large additional inter-tidal areas also covered under MHVM. Further, the coastal areas associated with wetlands such as Mudflats, mangroves, marsh vegetation, coral reefs, and saltpans (Mahapatra et al. 2015) are the regions recorded under the higher area MHVM. The maximum extent of MHVM was recorded in the Gulf of Kuchchh and on the eastern coasts of the Gulf of Khambat. Rest of the area along the open coast, the extent of MHVM is less due to comparatively elevated coasts. However, the coincidence of habitation areas with MHVM needs to be looked into cautiously to understand the actual vulnerability of the coastal communities.

Table 4. Area of MHVM recorded at each district and their percentage with respect to the district's geographic area along the Gujarat coast

District	MHVM Area (sq. km)	Percentage
Ahmedabad	85.14	1.22
Amreli	147.77	2.10
Anand	64.40	2.11
Baruch	1061.74	22.37
Bhavnagar	102.64	1.58
Devbhumi Dwaraka	520.62	13.01
Gir Somnath	184.77	7.25
Jamnagar	682.46	11.99
Junagadh	11.16	0.19
Kachchh	5869.29	15.00
Morbi	368.47	7.69
Navsari	284.23	13.37
Patan	214.33	3.85
Porbandar	318.70	14.30
Surat	422.59	10.12
Surendranagar	57.69	0.65
Valsad	104.47	3.67
Daman	3.72	5.39
Diu	21.02	56.05
Total	**10525.21**	

5.2. MAHARASHTRA

Coastal zones of the Maharashtra coast are exposed to oceanogenic hazards represented as MHVM, as shown in Figure 8. A total of 1733.8 km^2 coastal area recorded under MHVM.

Figure 8. MHVM map of Maharashtra coast

MHVM areas in northern Maharashtra extend to larger extents covering the districts of Raygad, Mumbai City, Sub Urban Mumbai and Palghar districts, suggesting higher vulnerability. The coastal areas of the Ratnagiri and Sindhudurg recorded fewer MHVM areas as they are low vulnerable. The spatial statics of the MHVM suggests that the maximum area recorded in Raygad with 777.15 km^2, followed by Palghar, Sindhudurg and Ratnagiri with an area of MHVM 409.17, 154.8 and 147.53 km^2, respectively. Whereas, the percentage of the area regarding the district's geographic area Mumbai city and Sub Urban Mumbai districts was recorded as the highest with 37.29 and 25.19 percent, respectively (Table 5).

Table 5. Area of MHVM recorded at each district and their percentage with respect to the district's geographic area along the Maharashtra coast

District	MHVM Area (sq. km)	Percentage
Mumbai City	23.13	37.29
Palghar	409.17	8.03
Ratnagiri	147.53	1.83
Raygad	777.15	11.48
Sindhudurg	154.80	3.10

Sub Urban Mumbai	105.30	25.19
Thane	116.72	2.82
Total	1733.8	

It was observed that the northern coasts of the state are more exposed, covering a large area under MHVM. These areas are experiencing higher inundation during the hazards that generate inundation. It was evident that the Mumbai city and suburban areas have experienced an extensive inundation during floods in the recent past. Further, the wide creaks and estuaries in the northern regions also allow additional inundation during the events, making these areas more vulnerable. On the contrary, Maharashtra's middle and southern coasts are less vulnerable due to the elevated coasts associated with cliffs (INCOIS, 2012). The estuaries in the southern parts are narrow and allow less inundation in the vicinity of these creeks.

5.3. GOA

The maritime state of Goa consists of two districts recorded 240.75 km^2 MHVM area, as shown in Figure 9.

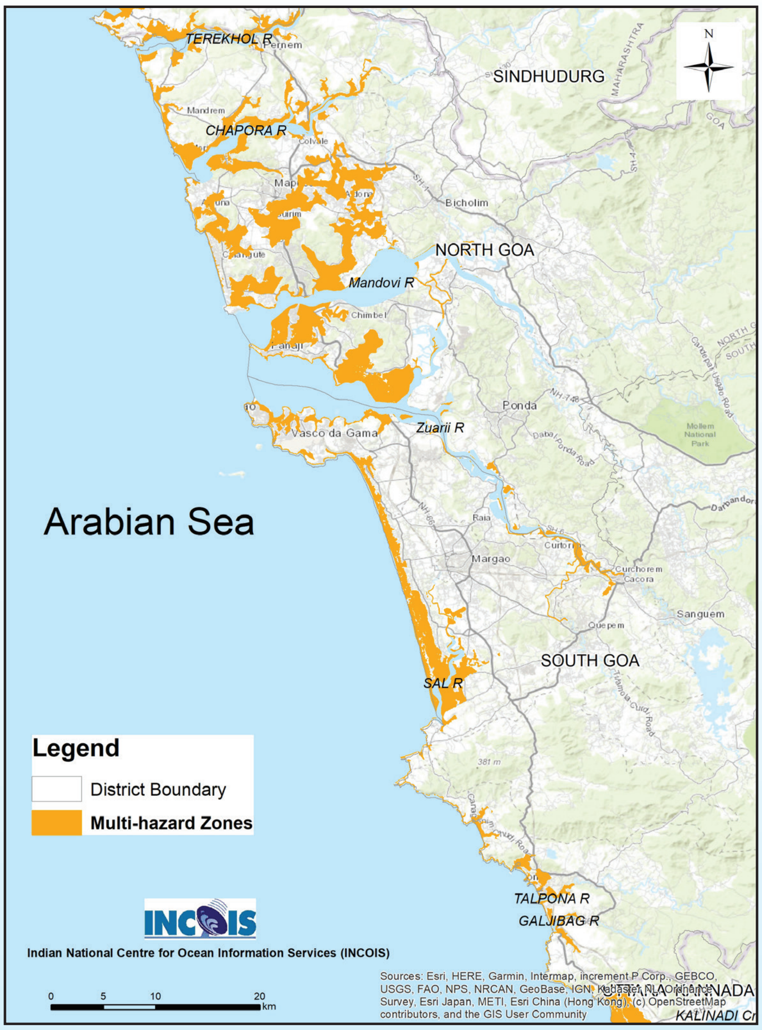

Figure 9. MHVM map of Goa Coast

The MHVM recorded 183.43 km^2, with 10.71 percent of the North Goa district's area being more vulnerable when compared to South Goa. In contrast, the South Goa district recorded a 57.32 km^2 area of MHVM with 2.98% (Table 6). The higher MHVM area was recorded in North Goa due to the Mandovi-Zuari estuary system with a wide estuary mouth. This suggests vulnerability in the vicinity of the estuary-creek system. Fortunately, the open coasts in North Goa recorded less MHVM area. South Goa in the southern parts also recorded large areas. Notably, open coasts along North Goa have recorded more areas under MHVM along the Margao urban coasts being vulnerable.

Table 6. Area of MHVM recorded at each district and their percentage with respect to the district's geographic area along the Goa coast

District	MHVM Area (sq. km)	Percentage
North Goa	183.43	10.71
South Goa	57.32	2.98
Total	240.75	

5.4. KARNATAKA

Karnataka comprises a coastline length of 320 km covering the Uttara Kannada, Udupi and Dakshina Kannada recorded MHVM area of 461 km^2. The MHVM map of the Karnataka coast is provided in Figure 10.

Figure 10. MHVM map of Karnataka Coast

The extent of MHVM along the open coasts is narrow, and the more extensive hinterland inundations were observed along the vicinity of the Kollur and Sita rivers in the Udupi district. The spatial extent of the MHVM was recorded maximum in the Udupi district, covering 246.74 km^2 with 6.93% of the district's area (Table 7). In comparison, Uttara Kannada and Dakshina Kannada districts were recorded as 161 and 53.42 km^2, comprising 1.59 and 1.1 % of the district's area, respectively. Overall, the Udupi district shows high vulnerability compared to the other two districts.

Table 7. Area of MHVM recorded at each district and their percentage with respect to the district's geographic area along the Karnataka coast

District	MHVM Area (sq. km)	percentage
Dakshina Kannada	53.42	1.10
Udupi	246.74	6.93
Uttara Kannada	161.30	1.59
Total	461.46	

5.5. KERALA

The MHVM map of the Kerala coast is provided in Figure 11, recording the total 1539.32 km^2 of the area under MHVM.

Figure 11. MHVM map of Kerala Coast

The MHVM areas depicting the coastal exposure along the Kerala coast were mostly constrained to the open coasts and in the vicinity of the creeks/river extending towards the hinterland. At the same time, a large area was exposed on the Ernakulam and Alappuzha coast around Vembanad lake, associated with many creeks systems. MHVM areas recorded in coastal districts are provided in Table 8 reveals the maximum area recorded in the Alappuzha district covering 440.37 km^2 with 30.29% of the district's area. Followed by Ernakulam, Kannur, Malappuram and Kozikode records 355.72, 171.07, 107.61 and 93.11 km^2 constitute 11.42, 5.75, 3 and 3.94 % respectively. Mahe is a union territory covered 0.76 km^2 area under MHVM with 8.48 % of the area.

Table 8. Area of MHVM recorded at each district and their percentage with respect to the district's geographic area along the Kerala coast

District	MHVM Area (sq. km)	percentage
Alappuzha	440.37	30.29
Ernakulam	355.72	11.42
Kannur	171.07	5.75
Kasaragod	79.18	3.97
Kollam	70.99	2.78
Kottayam	75.01	3.33
Kozhikode	93.11	3.94
Malappuram	107.61	3.00
Pattanamthitta	0.24	0.01
Thiruvananthapuram	65.52	2.90
Trissur	79.74	2.60
Mahe	0.76	8.48
Total	1539.32	

5.6. TAMIL NADU

The distribution of MHVM areas recorded along the Tamil Nadu coast is provided in Figure 12. A total of 5021.07 km^2 area of coastal zones of the state falls under MHVM and are exposed to oceanic hazards.

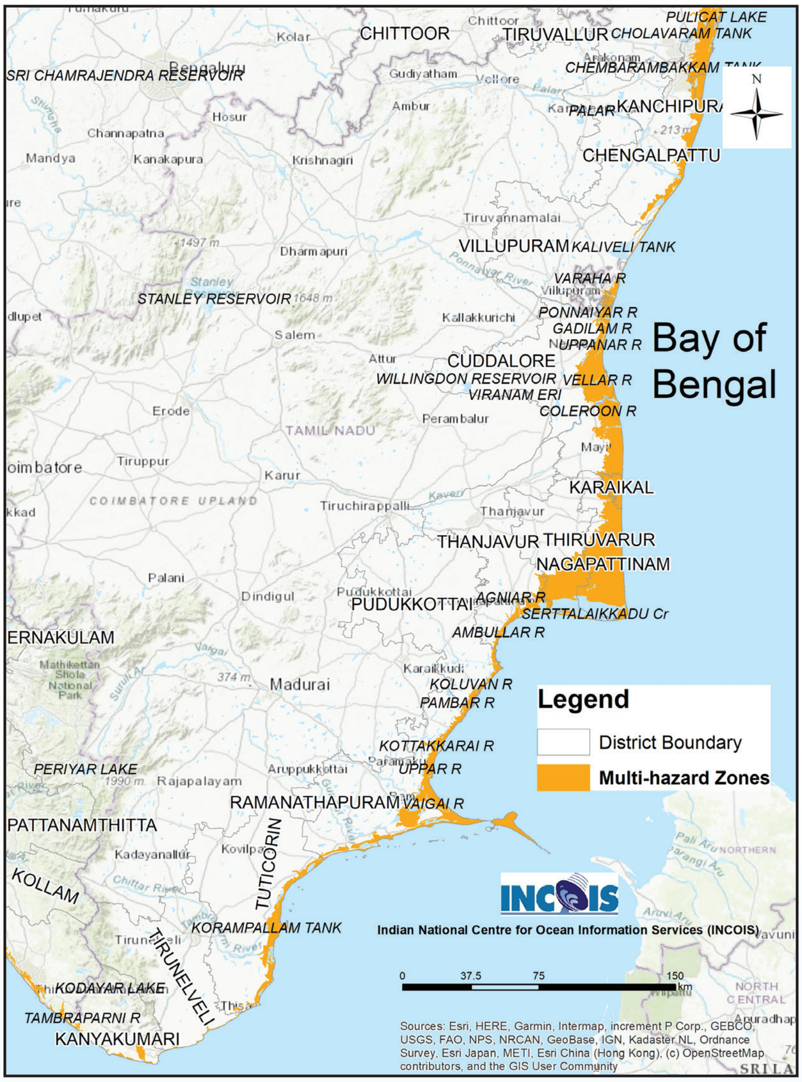

Figure 12. MHVM map Tamil Nadu coast

It was observed that the large extent of MHVM recorded at Nagapattinam, Puducherry, followed by Chennai, Toothukudi and Ramanathapuram coasts reveal the high exposure areas. The total area of MHVM recorded in each district is provided in Table 9. The highest area of, 1582.54 km^2 was recorded under MHVM in the Nagapattinam district, which constitutes 60.96% of the area of the district. The Ramanathapuram, Thiruvarur, Cuddalore, Thiruvallur and Toothukudi districts were recorded as 682.58, 544.15, 506.86, 399.31 and 269.02 km^2 areas, respectively. The highest 91.01% percentage of the Karaikal districts area was under MHVM, followed by Nagapattinam, Chennai, Thiruvarur and Puducherry districts, which were recorded at 60.96, 58.67, 23.72 and 21.63% of their district's area respectively.

Table 9. Area of MHVM recorded at each district and their percentage with respect to the district's geographic area along the Tamil Nadu coast

District	MHVM Area (sq. km)	percentage
Chengalpattu	220.22	8.09
Chennai	195.35	58.67
Cuddalore	506.86	13.60

Kanchipuram	72.06	4.14
Kanyakumari	40.00	2.30
Nagapattinam	1582.54	60.96
Pudukkottai	90.61	1.92
Ramanathapuram	682.58	16.23
Thanjavur	193.06	5.56
Thiruvarur	544.15	23.72
Tirunelveli	4.71	0.12
Tiruvallur	399.31	12.42
Tuticorin (Thoothukudi)	269.02	5.52
Villupuram	9.67	0.26
Karaikal	146.11	91.01
Puducherry	64.82	21.63
Total	5021.07	

5.7. ANDHRA PRADESH

The spread of the multi-hazard zone along the Andhra Pradesh coast is provided in Figure 13 below. A total of 10,180.72 km^2 coastal zone is recorded under multi-hazard vulnerability.

Figure 13. MHVM map of Andhra Pradesh Coast

The large extents of the coastal zones covered under the MHVM in the Krishna-Godavari delta coastal zones of West Godavari, East Godavari, Krishna, Prakasham and PottiSriramulu Nellore districts indicates the very exposed coasts. The district-wise statistics are provided in Table 10, showing the MHVM area and their percent with respect to the district's total area. The highest, 2875.9 km^2 area of MHVM was recorded in Krishna district, which constitutes 33.59% of the district's area. Followed by East Godavari, Potti Sriramulu Nellore, Guntur, Prakasam and West Godavari districts were recorded MHVM areas of 2875.9, 2004.62, 1728.16, 1263.21, 1032.47 and 870.03 km^2 respectively. However, coastal area Yanam is the union territory Under Puducherry districts situated along the Andhara Pradesh coast recorded 33.77 km^2 area under MHVM, which constitutes 91.43% of the total area. It was apparent that the coastal areas between the Krishna-Godavari delta and Pulicat lake in the south are more exposed and vulnerable when compared to the northern parts of the state.

Table 10. Area of MHVM recorded at each district and their percentage with respect to the district's geographic area along the Andhra Pradesh coast

District	MHVM Area (sq. km)	percentage
Chittoor	5.14	0.03
East Godavari	2004.62	15.92
Guntur	1263.21	11.32
Krishna	2875.9	33.59
Potti Sriramulu Nellore	1728.16	13.24
Prakasam	1032.47	5.97
Srikakulam	240.78	4.25
Visakhapatnam	116.73	1.04
Vizianagaram	9.91	0.17
West Godavari	870.03	10.71
Yanam	33.77	91.43
Total	10180.72	

5.8. ODISHA

The MHVM map of Odisha comprises ten coastal districts presented in Figure 14, covering an area of 8478.7 km^2 under MHVM exposed to Oceanogenic hazards.

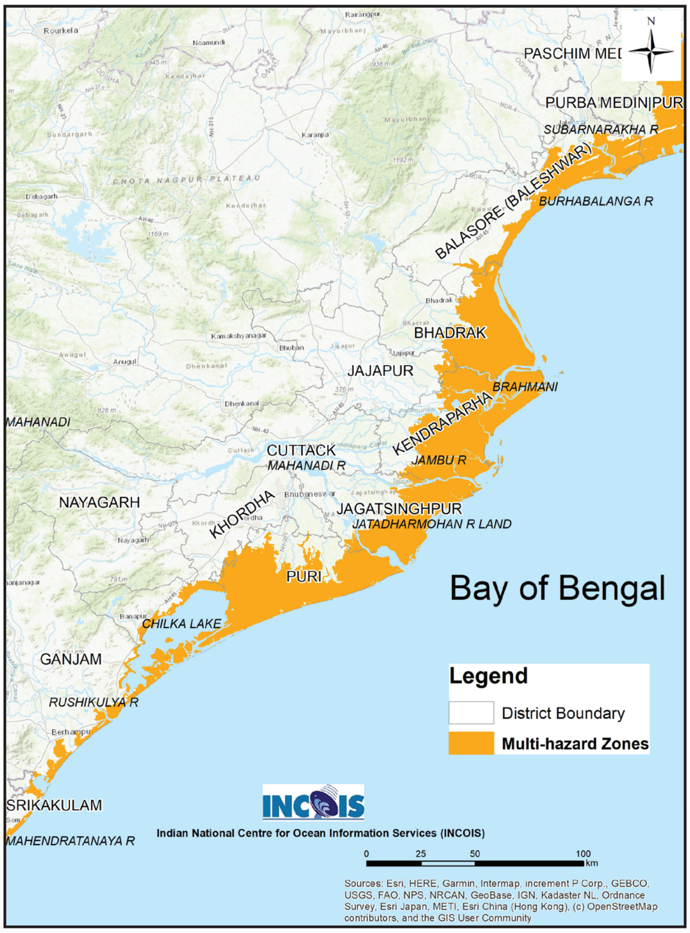

Figure 14. MHVM map of Odisha coast

it was observed that the large extent of MHVM was recorded in all the districts except Ganjam and parts of Balasore districts. This makes the state more vulnerable as large coastal areas are covered under MHVM when compared to the districts mentioned above. The spatial extents of MHVM recorded in each district, and their percentage is provided in Table 11. It was revealed that the maximum area of 2749.89 km^2 MHVM was recorded in the Puri district, which constitutes 81.91% of the area of the district, including Chilika Lake (the area of Chilika Lake is 1,165 km^2 as per https://whc.unesco.org/). The Kendraparha, Bhadrak, Jagatsinghpur and Balasore districts were recorded in 1898.64, 1251.88, 1000.67 and 980 km^2 areas, respectively, under MHVM. In the area beyond Carto-DTM, SRTM data were used in these areas, where large extents were reported in Odisha. These areas are required to be cautiously verified for the appropriate decisions and planning.

Table 11. Area of MHVM recorded at each district and their percentage with respect to the district's geographic area along the Odisha coast

District	MHVM Area (Sq. Km)	Percentage
Balasore (Baleswar)	980.00	27.36
Bhadrak	1251.88	51.82
Cuttack	28.21	0.76
Ganjam	279.34	3.44

Jagatsinghpur	1000.67	59.77
Jajapur	50.45	1.81
Kendraparha	1898.64	77.68
Khordha	241.34	8.68
Nayagarh	0.28	0.01
Puri	2747.89	81.91
Total	8478.7	

5.9. WEST BENGAL

The MHVM map of West Bengal comprises five districts is presented in Figure 15, covering an area of 10520.56 km^2 under MHVM exposed to Oceanogenic hazards.

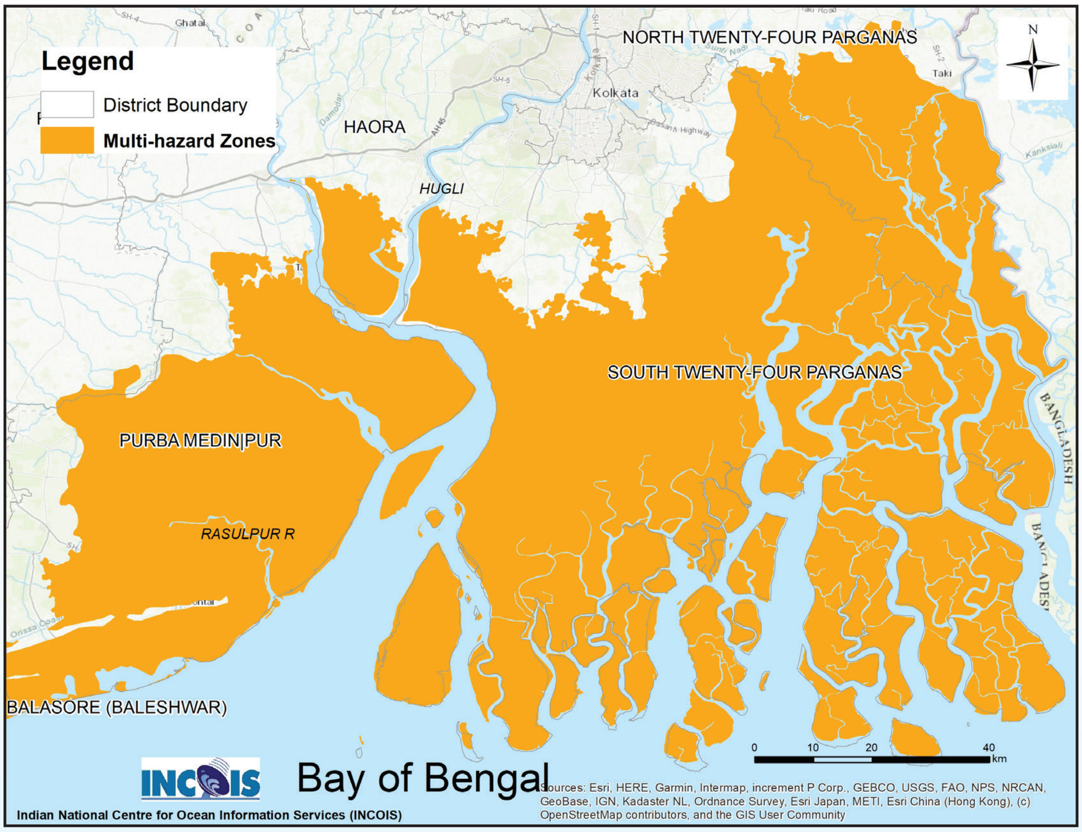

Figure 15. MHVM map of West Bengal coast

It was observed that most of the area of the district in Purba Medinipur and South 24 Paraganas districts are under MHVM and extend beyond these districts. The very large extent of the MHVM suggests the coastal zones of West Bengal are very low-lying and exposed to Oceanogenic hazards. The total area of MHVM and their percentage are provided in Table 12. The maximum area of 6383.31 km^2 MHVM was recorded in the South 24 Paraganas district, covering 86.48% of the district's total area, followed by the 2829.29, 1067.92 and 216.88 km^2 MHVM areas were recorded in Purba Medinipur, North 24 Parganas and Houra districts, respectively. In the area beyond Carto-DTM, SRTM data were used in this hinterland of West Bengal to avoid the abrupt ending of the MHVM due to the lack of high-resolution topographic data. These areas are required to be cautiously verified for the appropriate decisions and planning. The overview of the map itself indicates that the coastal zones of the state are highly exposed and vulnerable compared to the states previously discussed.

Table 12. Area of MHVM recorded at each district and their percentage with respect to the district's geographic area along the West Bengal coast

District	MHVM Area (sq. km)	percentage
Haora	216.88	15.35
North 24 Parganas	1067.92	27.72
Paschim Medinipur	23.16	0.38
Purba Medinipur	2829.29	74.27
South 24 Parganas	6383.31	86.48
Total	10520.56	

5.10. ANDAMAN AND NICOBAR

MHVM map of Andaman and Nicobar Islands covering the three districts is provided in Figure 16. The total area of MHVM recorded in this region was 900.34 km^2.

Figure 16. MHVM map of Andaman and Nicobar coast

It was observed that the MHVM areas were constrained to the open coasts, except for the large spread observed along the vicinity of the creeks in the Middle and North Andaman district. The spatial extents and the percentage of MHVM area in three coastal districts of Andaman and Nicobar are provided in Table 13. It was reported that the maximum area of 487.76 km^2 recorded in the Middle and North Andaman district constitutes 50.45% making this district more exposed. However, the south Andaman was recorded as 225.15 km^2 under MHVM, which constitute 36.27 percent of the area of the district. This is significant in this region because the region is more populated compared to other districts (as per Census of India, 2011). At the same time, the Nicobar district recorded 187.43 km^2 MHVM area, which constitutes 10.36 percent of the geographic area of Nicobar.

Table 13. Area of MHVM recorded at each district and their percentage with respect to the district's geographic area along the Andaman and Nicobar coast

District	MHVM Area (Sq. Km)	Percentage
Middle and North Andaman	487.76	50.45
South Andaman	225.15	36.27
Nicobar Islands	187.43	10.36
Total	900.34	

6. SUMMARY

Multi-hazard Vulnerability Mapping (MHVM) along the Indian Coast was carried out using the historical extreme water levels, historic shoreline change, sea level change, and high-resolution topographic data. After careful corrections, synthesis, and extensive GIS analyses, the multi-hazard vulnerability maps were finalized on 1:25,000 scale for the Indian mainland and Andaman & Nicobar Islands, where the topographic data is available. These maps represent the low-lying coastal areas that can experience inundation from oceanogenic hazards within 100 years of the return period.

These maps are highly accurate until the extent of the ALTM data used. The accuracy is slightly compromised beyond where other sources of topographic data from Carto-DTM, SRTM and ALOS-PALSAR data were used, as the sensitivity of the data is comparatively low. These maps can be further improved in these areas by using high-resolution data, better than sub-meter accuracy. The current study maps depict the exposure of the coastal zones to oceanogenic disasters. The exposed coastal elements, including coastal communities, need to be integrated to generate the socio-economic vulnerability of the coast to make better resilience plans.

The MHVM maps presented in this Atlas can be used as base coastal exposure information for disaster management and decision-making. These maps also provide vital inputs to disaster management organizations to make essential action plans for the National Coastal Mission to make a coastal community resilient against climate adversaries.

REFERENCES

Adams R., Western A.W., Law S., and Andersen S. (2009), The Development of an Integrated Modelling Framework for Assessing the Impacts of Land Use Change on Corner Inlet, 18Th World IMACS / MODSIM Congress, Cairns, Australia 13-17 July 2009.

Arjun S., Nair L., Sheela Shamji V. R. and Kurian N. P. (2010), Tidal Constituents in the Shallow Waters of the Southwest Indian Coast, Marine Geodesy, 33 (2), 206 - 217.

Crain C. M., Halpern B. S., Beck M. W., Kappel C. V. (2009) Understanding and managing human threats to the coastal marine environment. Ann N Y Acad Sci 1162:39-62. doi: 10.1111/j. 1749-6632.2009.04496.x.

Foreman (1977), Manual for Tidal Heights Analysis and Prediction. Pacific Marine Science Report 77-10.Victoria, B.C., Canada, Institute of Ocean Sciences, pp. 101.

Garg J. K., Singh T. S., Murthy T. U. R. (1998) Wetland of India, Space Application Centre (ISRO), Ahmedabad. Project Report on NationWide Wetland.

Grases A., Gracia V., García-León M., JueLin-Ye and Sierra J. P. (2020). Coastal Flooding and Erosion undera Changing Climate: Implications at a Low-Lying Coast (Ebro Delta). Water 2020,12, 346; doi:10.3390/w12020346.www.mdpi.com/journal/water.

Halpern B. S., Walbridge S., Selkoe K. A., (2008) A global map of human impact on marine ecosystems. Science, 319 (5865): 948-952.

INCCA. (2010). Climate change and India: A 4 9 4 Assessment—A sectoral and regional analysis for 2030s. INCCA: Indian Network for Climate Change Assessment, Ministry of Environment and Forests, Government of India.

INCOIS. (2012). Coastal vulnerability Atlas of India. Hyderabad: Indian National Centre for Ocean Information Services. ISBN NO-978-81-923474-0-0.

IPCC (2014). Climate Change 2014: Impacts, Adaptation, and Vulnerability. Part A: Global and Sectoral Aspects. Contribution of Working Group II to the Fifth Assessment Report of the Intergovernmental Panel on Climate Change [Field, C.B., V.R. Barros, D.J. Dokken, K.J. Mach, M.D. Mastrandrea, T.E. Bilir, M. Chatterjee, K.L. Ebi, Y.O. Estrada, R.C. Genova, B. Girma, E.S. Kissel, A.N. Levy, S. MacCracken, P.R. Mastrandrea, and L.L.White (eds.)]. Cambridge University Press, Cambridge, United Kingdom and New York, NY, USA, 1132 pp.

Jongman B., Ward P. J., Aerts JCJH (2012) Global exposure to river and coastal flooding: long term trends and changes. Glob Environ Chang 22(4): 823-835.

Krishnan P., Ananthan P. S., Purvaja R., Jeevamani J. J. J., Infantina J. A., Rao C.S., Anand A., Mahendra R. S., Sekar I., Kareemulla K., Biswas A., Sastry R. K., Ramesh R., (2019). Framework for mapping the drivers of coastal vulnerability and spatial decision making for climate-change adaptation: a case study from Maharashtra, India. Ambio 48, 192–212.

Krishnan R., Sanjay J., Gnanaseelan C., Mujumdar M., Kulkarni A., and Chakraborty S. (2020). Assessment of Climate Change Over the Indian Region: A Report of the Ministry of Earth Sciences (MoES), Government of India. Singapore: Springer. doi: 10.1007/978-981-15-4327-2.

Kumar T. S., Mahendra R. S., Nayak S., Radhakrishnan K., Sahu K. C. (2010) Coastal vulnerability assessment for Orissa state, east coast on India. J Coast Res 26(3):523–534.

Leary N., Adejuwon J., Bailey W., Barros V., Batima P., Caffera R. M., Cinvanno S., Conde C., Comarmond A. D., Sberbinin A. D., Downing T., Eakin H., Nyong A., Opondo M., Osman-Elassha B., Payet R., Pulbin F., Pulbin J., Ratnisri J., Sanjak E., Maltitz M. W., Yin Y., Ziervogel G. (2008) For whom the bell tolls: Vulnerability in a changing climate. In: Leary N., Conde C., Kulkarni J., Nyong A., Pulbin J. (eds) Climate change and vulnerability. Earthscan, London, pp 3–30.

Lee J. R., Maggini R., Taylor M. F.J., and Fuller R. A. (2015). Mapping the drivers of climate change vulnerability for Australia's threatened species. PLoS ONE. https://doi.org/10.1371/journal.pone.0124766.

Mahapatra M, Ramakrishnan R, Rajawat AS (2015) Coastal vulnerability assessment of Gujarat coast to sea level rise using GIStechniques: A preliminary study. J Coast Conserv 19:241–256.

Mahendra R. S., Mohanty P. C., Srinivasa Kumar T., Shenoi S. S. C., and Nayak S. (2010) Coastal Multi-hazard Vulnerability Mapping: A Case Study along the coast of the Nellore District, Andhra Pradesh, East Coast of India. Italian Journal of Remote Sensing: Vol. 42, Issue 3, pp. 67-76. https://doi.org/10.5721/ItJRS20104235.

Mahendra R. S, Mohanty P. C., Bisoyi H., Srinivasa Kumar T, Nayak S. (2011) Assessment and management of coastal multi-hazard vulnerability along the Cuddalore—Villupuram, east coast of India using geospatial techniques. Ocean and Coastal Management 54(4):302–311.

Mahendra, R. S., Mohanty, P. C., Francis, P. A., Sudheer Joseph, Balakrishnan Nair T. M. and Srinivasa Kumar T. (2021). Holistic approach to assess the coastal vulnerability to oceanogenic multi-hazards along the coast of Andhra Pradesh, India. Environ Earth Sci, 80, 651. https://doi.org/10.1007/s12665-021-09920-z.

Mohanty P. C., Mahendra R. S., Nayak R. K., Srinivasa Kumar T. (2017). Impact of sea level rise and coastal slope on shoreline change along the Indian coast. Natural Hazards. 89:1227–1238. DOI 10.1007/s11069-017-3018-9.

NCM. (2016). National Coastal Mission. New Delhi: Ministry of Environment, Forest and Climate Change, Government of India.

Piya L, Maharjan K. L., Joshi N. P. (2012) Vulnerability of rural households to climate change and extremes: Analysis of Chepang households in the mid-hills of Nepal. Selected paper prepared for presentation at the International Association of Agricultural Economics (IAAE) Triennial Conference, Foz do Iguacu, Brazil.

Pugh, D. T. (1987). Tides, surges and mean sea level, A Handbook for Engineers and Scientists, John Wiley & Sons Ltd., Chichester, 472 pp.

Rao, R. C. A., Raju B. M. K., Rao S.A.V.M., Rao K.V., Rao V.U.M., Ramachandran K., Venkateswarlu B., and Sikka A.K. (2013). Atlas on vulnerability of Indian agriculture to climate change.

Rishi P., Mudaliar R. (2014) Climate stress, behavioral adaptation and subjective well being in coastal cities of India. Am J Appl Psychol 2(1):13–21.

Sehgal V.K., Singh M.R., Jain N., and Pathak H. (2017). Climate change and variability: Mapping vulnerability of agriculture using Geospatial Technologies. In Agriculture under Climate Change: Threats, Strategies and Policies, ed. V.V. Belavadi, N.N. Karaba, and N.R. Gangadharappa, 74–79. Allied Publishers Pvt. Ltd.

Strauss B., Kulp S. (2014) New analysis shows global exposure to sea level rise, Climate Central, Retrieved from http://www.climatecentral.org/news/new-analysis-global-exposure-to-sea-level-rise-flooding-18066 on Dec 16 2014.

Unnikrishnan A. S., Manimurali M., Kumar R. (2010) Observed sea level rise, extreme events and future projections. Indian NetwClim Change Assess 4:47–66.

Wong P. P., Losada I. J., Gattuso J. P., Hinkel J., Khattabi A., McInnes K. L., Saito Y., Sallenger A. (2014). Coastal systems and low-lying areas. In: Climate Change 2014: Impacts, Adaptation, and Vulnerability. Part A: Global and Sectoral Aspects. Contribution of Working Group II to the Fifth Assessment Report of the Intergovernmental Panel on Climate Change [Field, C. B., Barros V. R., Dokken D. J., Mach K. J., Mastrandrea M. D., Bilir T. E., Chatterjee M.,Ebi K. L., Estrada Y. O., Genova R. C., Girma B., Kissel E. S., Levy A. N., Mac Cracken S., Mastrandrea P. R., White L. L. (eds.)]. Cambridge University Press, Cambridge, United Kingdom and New York, NY, USA, 361-409.

Zhang K., Gann D., Ross M., Robertson Q., Sarmiento J., Santana S., Rhome J. and Fritz C. (2019). Accuracy assessment of ASTER, SRTM, ALOS, and TDX DEMs for Hispaniola and implications for mapping vulnerability to coastal flooding. Remote Sensing of Environment 225: 290–306.